Earthq Eng & Eng Vib (2014) 13: 257-267 **DOI**: 10.1007/s11803-014-0228-y

Shaking table experimental study of recycled concrete frame-shear wall structures

Zhang Jianwei[1†], Cao Wanlin[1†], Meng Shaobin[1§], Yu Cheng[2‡] and Dong Hongying[1‡]

1. *College of Architecture and Civil Engineering, Beijing University of Technology, Beijing 100124, China*
2. *Department of Engineering Technology, University of North Texas, Denton, TX 76207, USA*

Abstract: In this study, four 1/5 scaled shaking table tests were conducted to investigate the seismic performance of recycled concrete frame-shear wall structures with different recycled aggregates replacement rates and concealed bracing detail. The four tested structures included one normal concrete model, one recycled coarse aggregate concrete model, and two recycled coarse and fine aggregate concrete models with or without concealed bracings inside the shear walls. The dynamic characteristics, dynamic response and failure mode of each model were compared and analyzed. Finite element models were also developed and nonlinear time-history response analysis was conducted. The test and analysis results show that the seismic performance of the recycled coarse aggregate concrete frame-shear wall structure is slightly worse than the normal concrete structure. The seismic resistance capacity of the recycled concrete frame-shear wall structure can be greatly improved by setting up concealed bracings inside the walls. With appropriate design, the recycled coarse aggregate concrete frame-shear wall structure and recycled concrete structure with concealed bracings inside the walls can be applied in buildings.

Keywords: recycled concrete; frame-shear wall; concealed bracings; shaking table test; nonlinear time-history response analysis

1 Introduction

In recent years, the Chinese building industry has been in a high speed development period. The demand of concrete results in the use of an extremely large amount of aggregates, and the excessive exploitation of natural sand and stone yielded serious damage to the environment. Meanwhile, significant volumes of construction waste were generated by demolition, renovation, and collapse of old buildings. It was estimated that approximately 200 million tons of waste concrete is currently produced annually in mainland China (Xiao *et al*., 2012). Making efficient use of this waste concrete from construction has become an urgent task for sustainability. One effective way to deal with waste concrete is to use it as aggregate to produce recycled concrete (Tam, 2009). Recycled concrete uses aggregates made from waste concrete which has been broken, classified and washed to partly or entirely replace natural aggregates, per Chinese Technical Code JGJ/T240-2011 (2011). Currently, the experimental studies on recycled concrete mainly focus on its material properties (Xiao *et al*., 2005; Xiao and Falkner, 2007; Tabsh and Abdelfatah, 2007; Casuccio *et al*., 2008; Belén *et al*., 2011). The studies on basic mechanical properties and seismic performance of recycled concrete structural members have made some progresses, such as the flexural behavior and shear capacity of beams (Xiao and Lan, 2006; Ajdukiewicz and Kliszczewicz, 2007; Sato *et al*., 2007; Fathifazl *et al*., 2011), compression behavior and seismic performance of columns (Xiao *et al*., 2006; Ajdukiewicz and Kliszczewicz, 2007; Bai *et al*., 2011) , seismic behavior of beam-column joints (Xiao and Zhu, 2005; Corinaldesi *et al*., 2011) , seismic behavior of shear walls (Cao *et al*., 2010a; Zhang *et al*., 2010), seismic behavior of frames (Sun *et al*., 2006), and seismic behavior of frame-shear wall structures (Cao *et al*., 2010b). However those experimental studies were carried out by means of static tests. There are only a few studies on the dynamic performance of recycled concrete structures. This paper presents the results of an experimental investigation of the dynamic performance of recycled concrete frame-shear wall structure through the use of shaking table tests. Four frame-shear wall

Correspondence to: Cao Wanlin, College of Architecture and Civil Engineering, Beijing University of Technology, Beijing 100124, China
Tel: +86-10-67392819; Fax: +86-10-67392819
E-mail: wlcao@bjut.edu.cn
[†]Professor ; [§]Master Student; [‡]Associate Professor

Supported by: National Science and Technology Support Program of China under Grant No. 2011BAJ08B02; Natural Science Foundation of Beijing under Grant No. 8132016; Beijing City University Youth Backbone Talent Training Project under Grant No. PHR201108009
Received January 10, 2013; **Accepted** November 1, 2013

structures were tested, and the research focuses on the influence of different recycled aggregate replacement ratios and concealed bracings.

2 Experimental details

2.1 Test specimens and test set-up

Four 1/5 scaled frame-shear wall models were labeled as FSW-0, FSW-1, FSW-2, and FSW-3. FSW-0 was made of normal concrete. FSW-1 was made of recycled coarse aggregate concrete. FSW-2 and FSW-3 were made of recycled coarse and recycled fine aggregate concrete. FSW-3 had reinforced concrete concealed bracings inside the shear walls (Cao *et al*., 2003, 2009). The beam was designed as a T-section in order to consider the concrete floor's contribution to the beam stiffness. The cantilever length on both sides was six times the floor thickness. The specimens all had the same dimensions and reinforcement layout. FSW-3 had concealed bracings inside the shear walls and the others did not. The dimensions and reinforcement layout of FSW-3 are shown in Fig. 1.

Φ8 steel bar was used for the longitudinal reinforcement of the concealed columns and concealed bracings in the shear wall as well as the frame columns. Φ6 steel bar was used for the longitudinal reinforcement of the frame beams. Φ4 galvanized iron wire was used for the stirrups of the columns, concealed bracings, beams, and the distributing bars in shear walls. The mechanical properties of the steel bar are listed in Table 1. The waste concrete was from a shopping mall demolition project in the Xidan area of Beijing, and the original concrete strength grade was C20. The test specimens were made by fine stone concrete and the maximum grain size of the coarse aggregate was 10 mm. The designed concrete strength grade for the specimens was C30. The mix proportion and mechanical properties of the concrete are listed in Table 2. The tests were conducted on the shaking table in the Key Laboratory of Urban Security and Disaster Engineering at the Beijing University of Technology. The table size is 3 m × 3 m. The similitude coefficient of models is provided in Table 3. The designed axial compression ratio of the shear wall was 0.1; therefore the added mass on the top of the specimen was 7 t. The gravity load trough was fixed to the model by bolts, and construction measures were taken to make sure that there was no relative displacement between the load trough and the specimen. To maintain in-plane stability of the structure in the test, four supporting poles were installed around the model and were connected with the load trough by slide bolts. The entire test device is shown in Fig. 2.

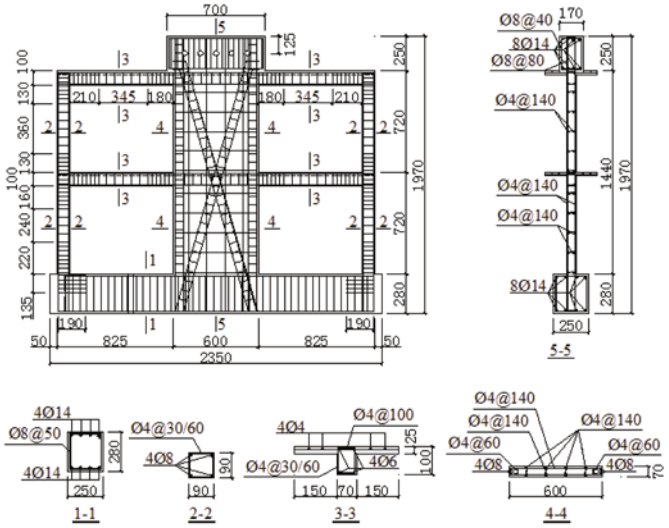

Fig. 1 Reinforcement details of FSW-3

Table1 Mechanical properties of steel bars

Diameter (mm)	Yield strength f_y (MPa)	Tensile strength f_u (MPa)	Elastic modulus E_s (MPa)
Φ4	312	352	1.79×10^5
Φ6	383	453	1.77×10^5
Φ8	338	493	1.98×10^5

Table 2 Mix proportions and mechanical properties of concrete

Specimen	Mix proportion(mass ratio)	Cubic compressive strength f_{cu} (MPa)
FSW-0	Cement : Natural sand : Natural stone : Water =1 : 1.25 : 2.5 : 0.5	35.5
FSW-1	Cement : Natural sand : Recycled coarse aggregate : Water =1 : 1.25 : 2.5 : 0.53	32.6
FSW-2 FSW-3	Cement : Recycled fine aggregate : Recycled coarse aggregate : Water =1 : 1.25 : 2.5 : 0.55	31.2

Table 3 Similitude coefficients

Physical quantity	Ratio of similitude (Model/Prototype)	Physical quantity	Ratio of similitude (Model/Prototype)
Strain ε	1	Stiffness K	1/5
Stress σ	1	Acceleration a	1
Elastic modulus E	1	Time t	$(1/5)^{1/2}$
Linear displacement x	1/5	Mass m	1/25

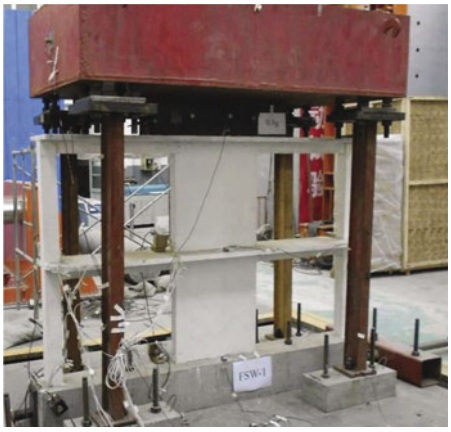

Fig. 2 Test setup

2.2 Test procedure and measurements

The El Centro N-S seismic wave was adopted as the input wave, and its peak ground acceleration (PGA) was modified to approximately 0.1 g, 0.15 g, 0.2 g, 0.3 g and so on. The actual PGA acquired by the accelerometer on the surface of the shaking table during the experimental procedure is shown in Table 4. According to the similitude coefficient of time, the time interval of the input seismic wave is 0.02 × 0.447 = 0.00894 s, and the duration is 50 × 0.447 = 22.361 s.

The natural frequency of models was measured through low amplitude white noise excitation. The test measurements also included the absolute acceleration response on each floor and on the position of the counterweight's centroid, each story's drift, the roof drift, the strain at the end of the longitudinal reinforcement in frame beams, frame columns and concealed columns of shear walls, and the strain at the end and in the middle of the concealed bracings' longitudinal reinforcement.

3 Experimental results and interpretation

3.1 Natural frequency of vibration

The change of the natural frequency can reflect variation characteristics of the specimens' stiffness. The test results indicated that as the damage level of the specimens increased, the natural frequency decreased gradually. That was because the cracks continually developed and the plastic deformations gradually increased during the course of tests. The natural frequency of each specimen measured in different stages is listed in Table 5. The results show that the initial natural frequency decreased when the recycled aggregates replacement ratio increased. Specimen FSW-1's initial natural frequency decreased by 10%, specimen FSW-2's decreased by 27%, and the initial natural frequency of FSW-3 was close to that of FSW-2. This indicates that the initial stiffness of the recycled aggregate concrete structures had a significant decrease, and the concealed bracings had no obvious effect on the structure's initial stiffness.

3.2 Acceleration response

The measured maximum absolute acceleration responses on the first floor for each specimen are summarized in Table 4. The comparisons of acceleration history responses among four specimens after cracking are shown in Fig. 3. The measured results of each specimen's absolute acceleration response in different stages indicate that: (1) Under the same peak acceleration of excitation, the acceleration response of FSW-1 is slightly higher than that of FSW-0, and the acceleration response of FSW-2 is much higher than that of FSW-0. After the concrete started cracking, the acceleration

Table 4 Test procedure and peak acceleration responses of first floor

Number	FSW-0		FSW-1		FSW-2		FSW-3	
	Peak acceleration of shaking table (g)	Peak acceleration response of first floor (g)	Peak acceleration of shaking table (g)	Peak acceleration response of first floor (g)	Peak acceleration of shaking table (g)	Peak acceleration response of first floor (g)	Peak acceleration of shaking table (g)	Peak acceleration response of first floor (g)
1	0.119	0.092	0.120	0.132	0.125	0.149	0.144	0.152
2	0.173	0.151	0.179	0.186	0.175	0.224	0.145	0.175
3	0.231	0.227	0.193	0.186	0.192	0.234	0.195	0.312
4	0.281	0.384	0.245	0.328	0.286	0.433	0.248	0.374
5	0.372	0.403	0.330	0.34	0.326	0.474	0.430	0.636
6	0.440	0.449	0.435	0.416	0.388	0.475	0.431	0.649
7	0.495	0.49	0.497	0.598	0.437	0.506	0.566	0.739
8	0.579	0.667	0.586	0.621	0.583	0.804	0.647	0.922
9	0.743	0.775	0.710	0.767	0.848	1.028	0.857	0.982
10	0.796	0.953	0.925	0.966	1.034	2.023	0.921	1.052
11	1.034	1.066	1.119	1.167	1.147	2.398	1.007	1.071
12	1.037	1.084	1.162	1.342	1.244	---	1.152	1.422
13	1.339	1.289	1.398	1.685	1.323	---	1.189	1.428
14	1.487	1.418	1.465	1.726			1.322	2.028
15	1.843	2.145					1.416	2.398

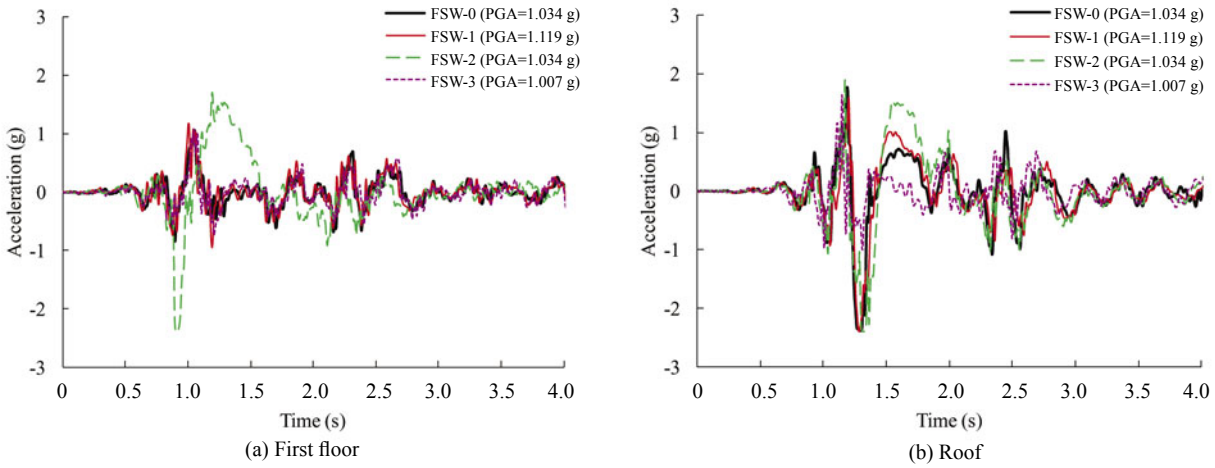

(a) First floor (b) Roof

Fig. 3 Acceleration history response of specimens after cracking

response of FSW-3 decreased significantly compared with that of FSW-2; (2) When initial cracks appeared, as shown in Table 5, the shaking table's peak acceleration for FSW-1 and FSW-2 was 31.3% and 37.7% lower than FSW-0, respectively, and FSW-3 was 41.7% lower than FSW-2. This shows that the seismic performance of the recycled coarse and recycled fine aggregate concrete structures was weaker than the normal aggregate concrete structure; however, their performance can be significantly improved by installing concealed bracings.

3.3 Displacement response

The measured results of each specimen's maximum story drift and roof drift in different stages are listed in Table 6. The drift history responses after the occurrence of cracks are shown in Fig. 4.

The test results show that: (1) Under the same peak acceleration of excitation, the displacement response increases as the recycled aggregates replacement ratio increases, and the displacement response after cracking decreases significantly in the structure with the concealed bracings. This is because the lateral stiffness of the recycled concrete frame-shear wall structure decreases with the growth of the recycled aggregates replacement ratio, and after the concrete starts cracking, the concealed bracings effectively maintain the lateral stiffness by restricting the development of diagonal cracks; (2) When the drift angle of the first story reaches 1/100, the shaking table's peak acceleration for FSW-1 and FSW-2 was 20.5% and 32.5% lower than FSW-0, respectively, and FSW-3 was 13.8% greater than FSW-2. This indicates that the earthquake resistance capacity of the recycled concrete frame-shear wall structure decreases as the recycled aggregates replacement ratio increased, and can be further enhanced by installing concealed bracings in the shear wall.

3.4 Base shearing force response

Under different excitation, the maximum nominal base shearing force of each specimen at the moment t, $F_i(t)_{\max}$, can be determined as follows:

$$F_i(t)_{\max} = \left|-ma_i(t)\right|_{\max} \tag{1}$$

where m is the centralized mass on the roof of the model, and a_i is the centroid acceleration for the i time excitation. The maximum values of the base shearing force are tabulated in Table 7. It can be concluded from Table 7 that under the same excitation, the maximum nominal base shearing force of the recycled coarse and recycled fine aggregate concrete structure is larger than that of a normal concrete structure, but it can be significantly decreased by installing concealed bracings in the shear wall.

Table 5 Test result of natural frequency

FSW-0		FSW-1		FSW-2		FSW-3	
Test procedure	f(Hz)	Test procedure	f(Hz)	Test procedure	f(Hz)	Test procedure	f(Hz)
Before wave excitation	5.86	Before wave excitation	5.27	Before wave excitation	4.25	Before wave excitation	4.32
After 0.281 g wave excitation(crack occurred)	5.23	After 0.193 g wave excitation (crack occurred)	4.96	After 0.175 g wave excitation (crack occurred)	3.96	After 0.248 g wave excitation (crack occurred)	3.98
After 0.440 g wave excitation	4.91	After 0.435 g wave excitation	4.69	After 0.437 g wave excitation	3.87	After 0.430 g wave excitation	3.92
After 0.743 g wave excitation	4.64	After 0.710 g wave excitation	4.35	After 0.848 g wave excitation	3.53	After 0.857 g wave excitation	3.54
After 1.034 g wave excitation	4.59	After 1.119 g wave excitation	3.53	After 1.147 g wave excitation	3.52	After 1.189 g wave excitation	3.52
After 1.843 g wave excitation	3.53	After 1.465 g wave excitation	3.52	After 1.323 g wave excitation	3.44	After 1.416 g wave excitation	3.50

Table 6 Maximum drifts and drift angles of each specimen

FSW-0					FSW-1				
Input (g)	First floor (mm)	Roof (mm)	First floor drift angle	Roof drift angle	Input (g)	First floor (mm)	Roof (mm)	First floor drift angle	Roof drift angle
0.119	0.130	0.370	1/5552	1/3889	0.120	0.324	0.518	1/2221	1/2778
0.173	0.195	0.518	1/3702	1/2778	0.179	0.648	0.889	1/1110	1/1621
0.231	0.195	0.704	1/3702	1/2045	0.193	0.648	0.963	1/1110	1/1496
0.281	0.324	0.741	1/2221	1/1945	0.245	0.843	1.260	1/854	1/1143
0.372	0.519	1.112	1/1388	1/1295	0.330	1.038	1.482	1/693	1/972
0.440	0.713	1.445	1/1010	1/997	0.435	1.103	1.630	1/653	1/883
0.495	1.168	1.630	1/616	1/883	0.497	1.233	1.778	1/584	1/810
0.579	1.363	2.075	1/528	1/694	0.586	1.557	2.149	1/462	1/670
0.743	1.524	2.445	1/472	1/589	0.710	2.725	3.631	1/264	1/397
0.796	2.465	3.335	1/292	1/432	0.925	3.374	4.445	1/213	1/324
1.034	2.660	4.223	1/271	1/341	1.119	4.996	6.372	1/144	1/226
1.037	3.114	5.261	1/231	1/274	1.162	5.449	7.262	1/132	1/198
1.339	4.412	7.410	1/163	1/194	1.398	7.007	9.559	1/103	1/151
1.487	5.060	8.373	1/142	1/172	1.465	7.396	9.781	1/97	1/147
1.843	7.136	10.743	1/101	1/134					

FSW-2					FSW-3				
Input (g)	First floor (mm)	Roof (mm)	First floor drift angle	Roof drift angle	Input (g)	First floor (mm)	Roof (mm)	First floor drift angle	Roof drift angle
0.125	0.519	0.666	1/1388	1/2161	0.144	0.342	0.713	1/2106	1/2020
0.175	0.778	1.000	1/925	1/1440	0.145	0.513	0.951	1/1404	1/1514
0.192	0.941	1.112	1/765	1/1295	0.195	0.856	1.494	1/842	1/964
0.286	1.168	1.630	1/616	1/883	0.248	1.254	1.629	1/574	1/884
0.326	1.557	2.149	1/462	1/670	0.430	2.166	2.715	1/332	1/530
0.388	1.622	2.149	1/444	1/670	0.431	2.223	2.919	1/324	1/493
0.437	1.816	2.445	1/396	1/589	0.566	2.907	4.005	1/248	1/360
0.583	2.530	3.557	1/285	1/405	0.647	2.964	4.141	1/243	1/348
0.848	3.438	5.706	1/209	1/252	0.857	4.219	5.702	1/171	1/253
1.034	5.125	7.706	1/140	1/187	0.921	4.390	6.245	1/164	1/231
1.147	6.747	9.114	1/107	1/158	1.007	4.902	6.789	1/147	1/212
1.244	7.136	9.410	1/100	1/153	1.152	5.016	7.263	1/144	1/198
1.323	7.655	9.559	1/94	1/151	1.189	5.530	7.399	1/130	1/195
					1.322	6.784	8.893	1/106	1/162
					1.416	7.182	9.096	1/100	1/158

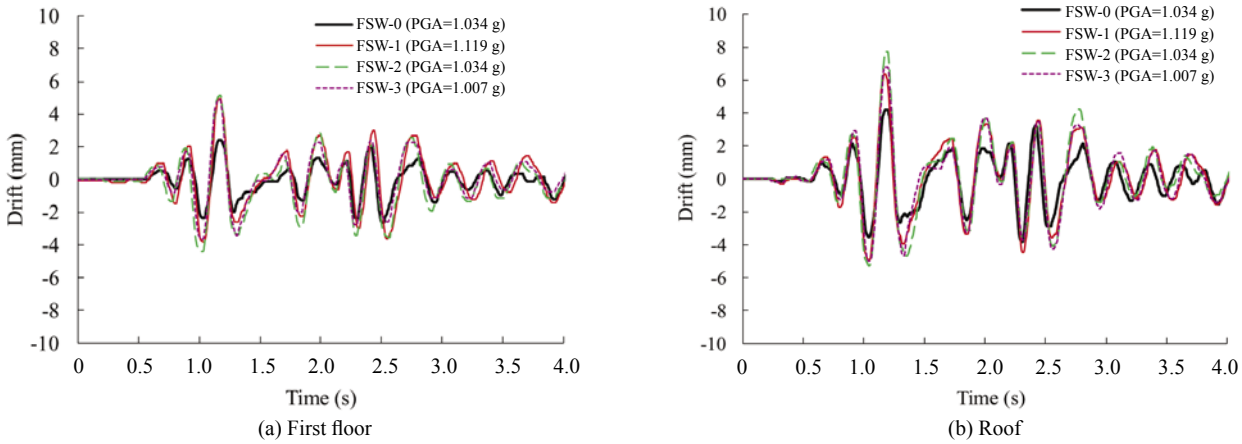

(a) First floor (b) Roof

Fig. 4 Drift history responses of specimens after cracking

Table 7 Maximum base shearing forces of each specimen

FSW-0		FSW-1		FSW-2		FSW-3	
Input (g)	*F* (kN)	Input (g)	*F* (kN)	Input (g)	*F* (kN)	Input (g)	*F* (kN)
0.119	8.95	0.120	12.45	0.125	14.78	0.144	15.95
0.173	12.74	0.179	19.44	0.175	22.06	0.145	21.11
0.231	21.11	0.193	20.53	0.192	25.19	0.195	33.56
0.281	24.97	0.245	29.70	0.286	37.71	0.248	44.12
0.372	38.07	0.330	33.20	0.326	46.37	0.430	69.67
0.440	45.94	0.435	37.86	0.388	47.68	0.431	76.66
0.495	48.70	0.497	44.63	0.437	52.20	0.566	92.67
0.579	59.62	0.586	54.74	0.583	77.53	0.647	103.37
0.743	72.80	0.710	84.52	0.848	115.90	0.857	113.71
0.796	105.85	0.925	109.41	1.034	181.76	0.921	116.77
1.034	173.77	1.119	173.99	1.147	---	1.007	119.53
1.037	174.06	1.162	196.33	1.244	---	1.152	128.05
1.339	203.62	1.398	---	1.323	---	1.189	141.66
1.487	---	1.465	---			1.322	203.68
1.843	---					1.416	---

3.5 Failure characteristics

In the FSW-0 model, after earthquake excitation with a PGA of 0.281 g, inclined cracks appeared at the joint areas between the shear walls and frame beams in both stories, and horizontal cracks occurred at the top of columns in the second story. After excitation with a PGA of 0.372 g, horizontal cracks occurred at the middle height of the concealed columns in both stories, and bending cracks started appearing at the ends of the beam in the second story. After excitation with a PGA of 0.579 g, bending cracks occurred at the beam ends and frame columns in the first story. After excitation with a PGA of 0.796 g, diagonal crossing cracks appeared at the 4/5 height region of the shear wall in the first story, vertical rebar at the bottom of concealed first story columns yielded, and one major diagonal crack occurred at the 3/4 height region of second story shear wall. After excitation with a PGA of 1.037 g, concrete peeled off at the joint between shear wall and frame beam in the first story, and longitudinal rebar in the ends of the first story's frame beam yielded. After excitation with a PGA of 1.339 g, the cracks in the shear walls went across the entire wall width, long cracks appeared at the first story's shear wall base, the maximum crack width of the shear wall was 0.2 mm after the test, and the vertical rebar at the bottom of the first story columns yielded. After excitation with a PGA of 1.487 g, the concrete at the bottom corners of the first story shear wall crushed, and the maximum crack width of the shear wall was 0.4 mm after the test.

In the FSW-1 model, after excitation with a PGA of 0.193 g, inclined cracks appeared at the joint area between the beams and the shear walls at both stories, and horizontal cracks appeared at the column top area in the second story. After excitation with a PGA of 0.710 g, inclined cracks appeared in both directions on the bottom 2/3 portion of the first story shear wall, vertical rebar in the bottom of concealed columns yielded in the first story, and short cracks occurred on the corners of the second story shear walls. After excitation with a PGA of 0.925 g, the inclined cracks on the first story shear walls formed a main diagonal crack field, U shape cracks appeared at the joint between the first story shear wall and beams where the concrete peeled off, and longitudinal rebar in the ends of the first story beams yielded. After excitation with a PGA of 1.162 g, concrete at the bottom corners of the first story shear wall crushed, the maximum crack width of the shear wall reached 0.2 mm after the test, and the vertical rebar in the bottom of the first story columns yielded. After excitation with a PGA of 1.398 g, the cracks in the first story shear wall appeared across the entire wall, concrete at the first shear wall's bottom corners crushed and peeled off, longitudinal cracks appeared along the shear wall base, and the cracks in the second story shear wall expanded and formed major crack fields.

In the FSW-2 model, after excitation with a PGA of 0.175 g, vertical cracks appeared at the joint areas between the beams and shear walls at both stories, and horizontal cracks appeared at the top area of the columns at the second story. After excitation with a PGA of 0.326 g, short inclined cracks appeared on the second story shear wall, and vertical cracks appeared on the beams with the 1/3 span from the shear wall. After excitation with a PGA of 0.583 g, two-direction inclined cracks occurred on the first story shear wall at 1/3 height, and the vertical rebar in the bottom of the concealed columns at the first story yielded. After excitation with a PGA of 0.848 g, the inclined cracks on the story shear walls at both stories expanded and more cracks occurred, the concrete peeled off at the joint between the beam and column at first story, and the vertical rebar in the first story beams yielded. After excitation with a PGA of 1.034 g, the maximum crack width of the shear wall reached 0.2 mm after the test, and the vertical rebar at the column bottom

in the first story yielded. After excitation with a PGA of 1.244 g, the main cracks in the first story shear wall appeared across the entire wall width, concrete peeled off at the bottom corners of the first story shear wall, and the maximum crack width of the shear wall reached 0.4 mm after the test.

In the FSW-3 model, after excitation with a PGA of 0.248 g, vertical cracks appeared on the joint areas between the beams and shear walls at both stories, horizontal cracks appeared at the top of the second story columns, and the ends of the second story beams showed bending cracks. After excitation with a PGA of 0.431 g, inclined cracks appeared in the middle of the second story shear wall. After excitation with a PGA of 0.647 g, inclined cracks appeared in the middle of the first story shear wall and in the bottom of the second story shear wall, longitudinal rebar of the concealed bracings yielded, and vertical cracks appeared on the first story beams within 20 cm from the shear wall. After excitation with a PGA of 0.857 g, vertical rebar in the concealed columns of the first story yielded. After excitation with a PGA of 1.152 g, long cracks crossed the entire base of the first story shear wall, the maximum crack width of the shear wall reached 0.2 mm after the test, concrete peeled off at the joint area between the beams and shear wall on the first story, and the longitudinal rebar of the first story beams yielded. After excitation with a PGA of 1.322 g, concrete at the bottom corners of the first story shear wall crushed and peeled off, and the maximum crack width of the shear wall reached 0.4 mm after the test.

When the first story drift angle of the specimens reached the limit value of 1/100 in the Chinese Code GB50011 (2010), the failure mode of the first story shear wall of each specimen is shown in Fig. 5. The final failure mode of each specimen is shown in Fig. 6. The

(a) FSW-0 (b) FSW-1 (c) FSW-2 (d) FSW-3

Fig. 5 Failure mode of the first story shear wall with 1/100 first story drift angle

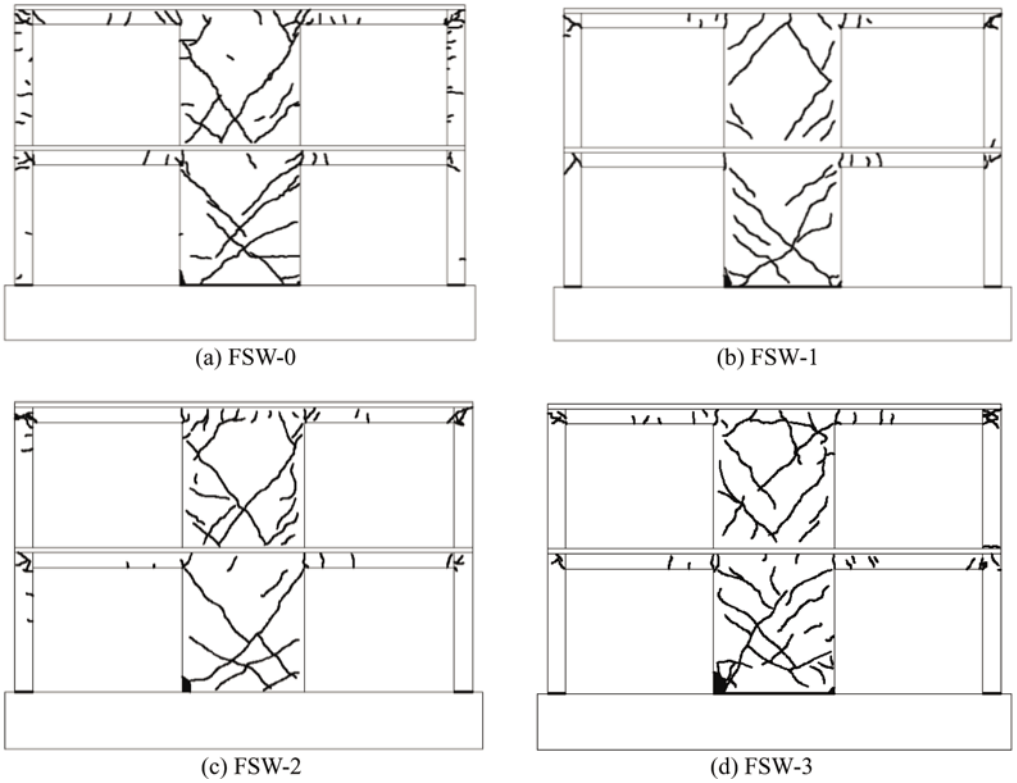

(a) FSW-0 (b) FSW-1

(c) FSW-2 (d) FSW-3

Fig. 6 Final failure mode of specimens

failure characteristics can be summarized as follows.

(1) The failure characteristic for all specimens is that shear failure first occurs in the shear walls and then plastic hinges are formed successively in the end of the frame beams and columns, and this embodies the design ideas of "two seismic fortification lines" and "strong column-weak beam" in the frame-shear wall structure.

(2) Compared with specimens FSW-2 and FSW-3, diagonal cracks in the walls of the specimens FSW-0 and FSW-1 appear relatively late, but the initial cracks are much longer and develop rapidly into main cracks. FSW-2 and FSW-3's initial diagonal cracks of the walls are shorter, and the process of the initial cracks' developing into main cracks is longer when compared to FSW-0 and FSW-1.

(3) When the shear wall failure occurs, cracks in FSW-0-FSW-2 are concentrated in the lower part of the wall and are less than those of FSW-3, but they are wider. However, because of the effect of the concealed bracings in the walls, the development of cracks in the walls of FSW-3 is greatly restricted, and are concentrated in the middle part of the wall.

(4) When the maximum width of the wall cracks reaches 0.2 mm, the shaking table's peak acceleration in FSW-1 and FSW-2 is decreased by 13.2% and 22.8%, respectively, when compared with FSW-0. The shaking table's peak acceleration for FSW-3 is increased by 11.4% when compared with FSW-2.

(5) When the maximum width of the wall cracks reaches 0.4 mm, the shaking table's peak acceleration for FSW-1 and FSW-2 is decreased by 1.5% and 16.3% when compared with FSW-0, and is increased for FSW-3 by 6.3% when compared with FSW-2.

These observations indicate that the seismic capacity of specimens FSW-1 and FSW-3 is closer to FSW-0.

4 Elastic-plastic finite element simulation

Simulation analysis of each specimen was conducted using finite element software ABAQUS. The ABAQUS models were based on measured mechanical properties of concrete and steel bars. Steel bars were defined as isotropic elastic-plastic material, and its stress-strain curve relation is shown in Eq. (2). A damage-plasticity model was used for normal and recycled concrete, and the uniaxial tension and compression stress-strain curve equations from the current Chinese Code GB50010 (2010) were used for the constitutive relation, as shown in Eq. (3) and Eq. (4).

$$\sigma_s = \begin{cases} E_s \varepsilon_s & \varepsilon_s \le \varepsilon_y \\ f_y & \varepsilon_s > \varepsilon_y \end{cases} \tag{2}$$

$$\sigma = (1\text{-}d_t) E_c \varepsilon \tag{3}$$

$$\sigma = (1\text{-}d_c) E_c \varepsilon \tag{4}$$

where σ_s is the steel bar stress; f_y is the yield strength of the steel bar; ε_s is the steel bar strain; ε_y is the yield strain of the steel bar; E_s is the elastic modulus of the steel bar; σ is the concrete stress; ε is the concrete strain; d_t is the damaged parameter of concrete in extension, d_c is the damaged parameter of concrete in compression, and E_c is the elastic modulus of concrete.

The damaged parameter of concrete in extension or compression is obtained by Eq. (5) and Eq. (6).

$$\text{When } x \le 1, \quad d_t = 1\text{-}\rho_t[1.2\text{-}0.2x^5] \tag{5a}$$

$$\text{When } x > 1, \quad d_t = 1\text{-}\rho_t/[\alpha_t(x\text{-}1)^{1.7}+x] \tag{5b}$$

where $x = \varepsilon/\varepsilon_t$; $\rho_t = f_t^* /(E_c \varepsilon_t)$; f_t^* is the uniaxial tensile strength; and ε_t is the corresponding peak tensile strain with f_t^*. α_t is the parameter at the descent stage of the concrete tensile stress-strain curves and its value can be obtained from the Chinese Code GB50010 according to f_t^*.

$$\text{When } x \le 1, \quad d_c = 1\text{-}\rho_c n/(n\text{-}1+x^n) \tag{6a}$$

$$\text{When } x > 1, \quad d_c = 1\text{-}\rho_c/[\alpha_c (x\text{-}1)^2+x] \tag{6b}$$

where $x = \varepsilon/\varepsilon_c$; $\rho_c = f_c^* /(E_c \varepsilon_c)$; $n = E_c \varepsilon/(E_c \varepsilon\text{-} f_c^*)$; f_c^* is the uniaxial prismatic compression strength; ε_c is the corresponding peak compression strain with f_c^*; α_c is the parameter at the descent stage of concrete compression stress-strain curves and its value can be obtained from the Chinese Code GB50010 (2010) according to f_c^*.

In the ABAQUS modeling, steel bars and concrete were separated, and T3D2 and C3D8R were, respectively, used for the element type of steel bars and concrete. The constraint relation of Embedded was used to simulate the interaction between the steel bars and concrete. The added mass on the top of the specimens was defined as Point mass, and was assigned to the central node of the loading beam to simulate the axial pressure and the inertial force generated by the added mass. Energy dissipation existed in the test, which was caused by internal and external factors, such us friction at connection joints and viscous internal friction of the material (Zhuang *et al*., 2009). In order to simulate the energy dissipation in the models, the material damping was defined in material property, and the damping coefficients were defined in the point mass definition. Mesh generation of the test specimen is shown in Fig. 7.

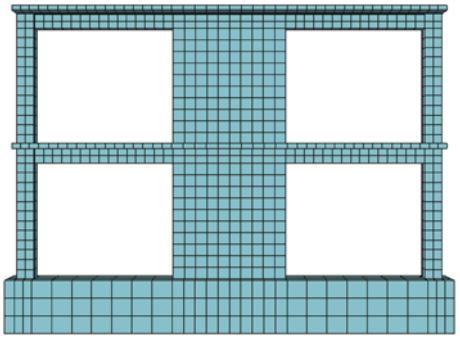

Fig. 7 Mesh generation of the model

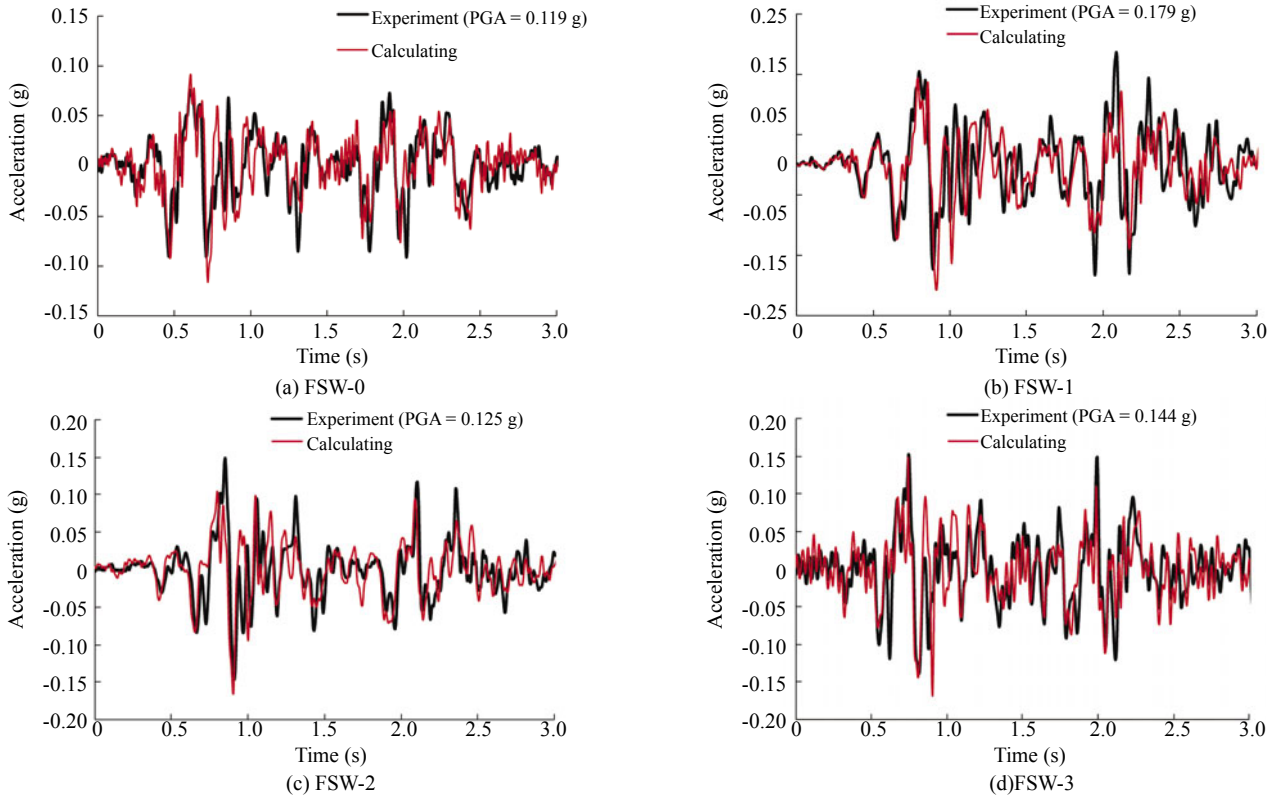

Fig. 8 Comparison of acceleration history response of the first floor in elastic stage

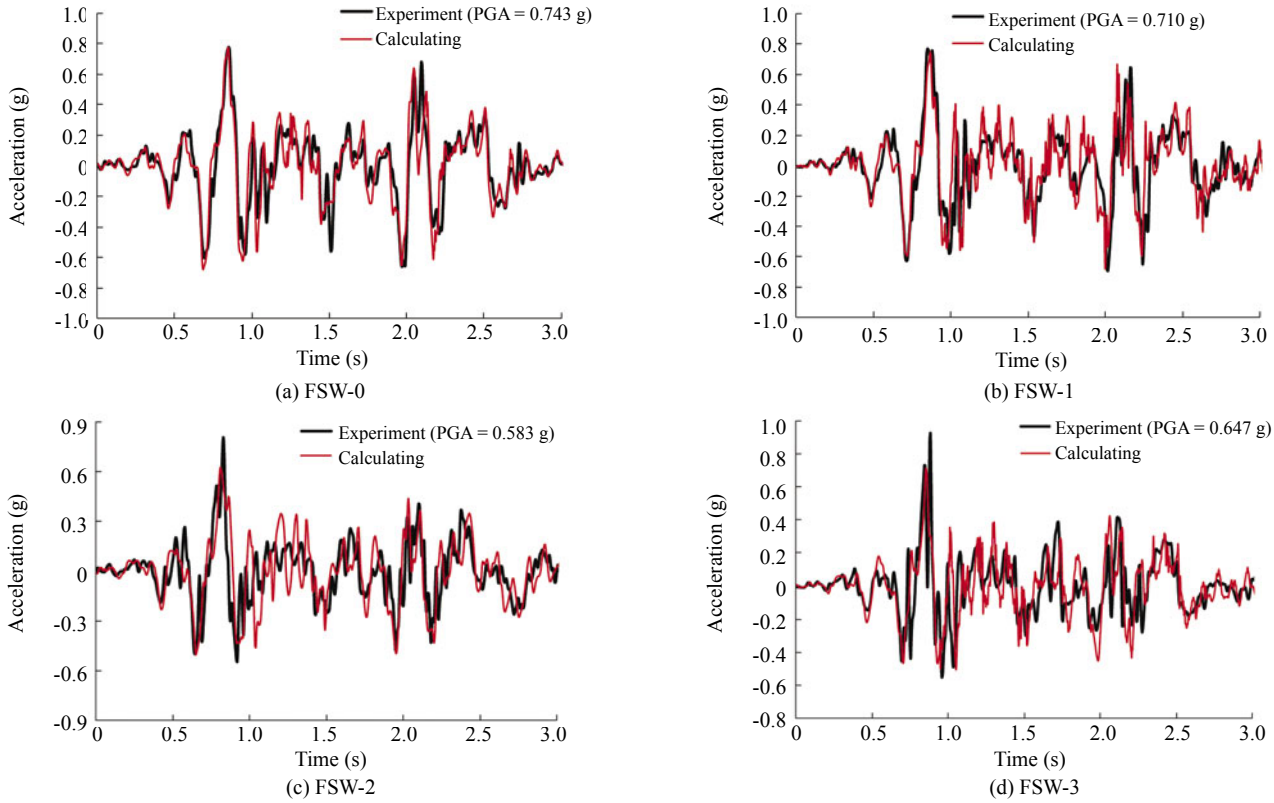

Fig. 9 Comparison of acceleration history response of the first floor in elastic-plastic stage

In the analysis process, the general static step was created first, and then the gravity load was applied on the whole model and was propagated in the latter steps. Then, an implicit dynamic step was created and measured acceleration boundary conditions were applied on the bottom surface of the foundation. The acceleration responses in the elastic and elastic-plastic stage were extracted from the analysis results, and were

compared with the test results. The comparison of each specimen's tested and simulated acceleration history responses of the first floor in the elastic and elastic-plastic stage is shown in Fig. 8 and Fig. 9.

According to the research results of Lubliner *et al.*, cracking initiates at points where the tensile equivalent plastic strain and the maximum principal plastic strain are positive (Wang and Chen, 2006). The tensile equivalent plastic strain of the specimen FSW-0 when cracking occurred is shown in Fig. 10. The figure shows that the tensile equivalent plastic strain in the junction of each story's wall and beam has a relatively large value, and the initial cracks just appear there according to the description in Section 3.5 of this paper. The tensile damage of FSW-0 in the plastic stage is shown in Fig. 11. Figure 11 shows that the tensile damage region of the second story's joint areas is wider than in the first story, and the degree of damage in the second story's joint areas is more severe than in the first story in the test.

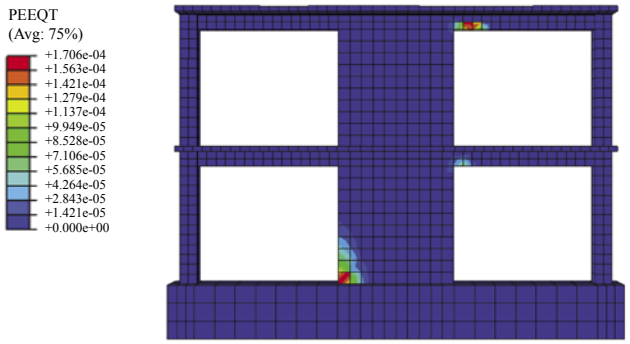

Fig. 10 Tensile equivalent plastic strain of specimen FSW-0 when cracking

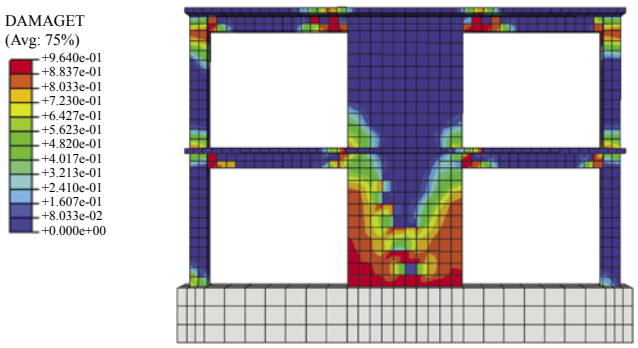

Fig. 11 Tensile damage of specimen FSW-0 in plastic stage

5 Conclusions

(1) The initial stiffness of the recycled concrete frame-shear wall structure is weaker than the normal concrete structure. The initial natural frequency decreases as the recycled aggregates replacement ratio increases. The concealed bracings do not have a significant effect on the model's initial stiffness.

(2) When initial cracks appear, the shaking table's peak acceleration of the recycled concrete frame-shear wall structure is lower than the normal concrete structure, and the reduced degree increases as the recycled aggregates replacement ratio increases. When the observed peak acceleration of the shaking table is basically the same, the acceleration response of the recycled coarse and recycled fine aggregate concrete structure is significantly greater than the normal concrete structure. The use of concealed bracings in shear walls can obviously reduce the acceleration response.

(3) When the observed peak acceleration of the shaking table is basically the same, the displacement response of the recycled concrete frame-shear wall structure is greater than the normal concrete structure. The displacement responses increase as the ratio of the recycled aggregates replacement increases. The use of concealed bracings in shear walls can reduce the displacement response.

(4) The failure mechanism of the recycled concrete frame-shear wall structure is essentially the same as the normal concrete structure. Under the same peak acceleration of the shaking table, the damage degree of the recycled coarse aggregate concrete structure is close to that of the normal concrete structure. The damage degree of the recycled coarse and recycled fine aggregate concrete structure is relatively severe. The concealed bracings in shear walls restrict the development of the cracks, and as a result, more cracks appeared with smaller width and concentrated in the middle part of the wall. The structure ductility can be improved.

(5) Compared with the normal concrete frame-shear wall structure, the seismic capacity of the recycled coarse aggregate concrete structure is weaker, but still meets the requirements of seismic design as per Chinese Code GB50011 (2010). The use of concealed bracings in shear walls can significantly improve the seismic capacity of the recycled concrete frame-shear wall structures and is suitable for use in recycled concrete structures. The numerical simulation analysis method for the normal concrete structures can be used for the recycled concrete frame-shear wall structures.

Acknowledgement

The authors are grateful for the funding provided by the National Science and Technology Support Program of China (2011BAJ08B02), the Natural Science Foundation of Beijing (8132016), and the Beijing City University Youth Backbone Talent Training Project (PHR201108009).

References

Ajdukiewicz AB and Kliszczewicz AT (2007), "Comparative Tests of Beams and Columns Made of Recycled Aggregate Concrete and Natural Aggregate

Concrete," *Journal of Advanced Concrete Technology*, **5**(2): 259–273.

Bai GL, Li C and Zhao HJ (2011), "Experimental Research on Seismic Behavior of Recycled Concrete Frame Columns," *Journal of Earthquake Engineering and Engineering Vibration*, **31**(1): 61–66. (in Chinese)

Belén GF, Fernando MA, Diego CL and Sindy SP (2011), "Stress-strain Relationship in Axial Compression for Concrete Using Recycled Saturated Coarse Aggregate," *Construction and Building Materials*, **25**(5): 2335–2342.

Cao WL, Dong HY and Zhang JW (2010a), "Study on Seismic Performance of RAC Shear Wall with Different Shear-span Ratio," *Proceedings of the second International Conference on Waste Engineering and Management*, Shanghai, China, pp. 652–660.

Cao WL, Xue SD and Zhang JW (2003), "Seismic Performance of RC Shear Wall with Concealed Bracing," *Advances in Structural Engineering*, **6** (1): 1–13.

Cao WL, Zhang JW, Yin HP and Chen JL (2010b), "Experimental Study on the Seismic Behavior of Recycled Concrete Frame-shear-wall Structure," *Engineering Mechanics*, **27**(SII):135–141. (in Chinese)

Cao WL, Zhao CJ, Xue SD and Zhang JW (2009), "Shaking Table Experimental Study of the Short Pier RC Shear Wall Structures with Concealed Bracing," *Advances in Structural Engineering*, **12** (2): 267–278.

Casuccio M, Torrijos MC, Giaccio G and Zerbino R (2008), "Failure Mechanism of Recycled Aggregate Concrete," *Construction and Building Materials*, **22**: 1500–1506.

Corinaldesi V, Letelier V and Moriconi G (2011), "Behaviour of Beam-column Joints Made of Recycled-aggregate Concrete under Cyclic Loading," *Construction and Building Materials*, **25**(4): 1877–1882.

Fathifazl G, Razaqpur AG, Burkan Isgor O, Abbas A, Fournier B and Foo S (2011), "Shear Capacity Evaluation of Steel Reinforced Recycled Concrete (RRC) Beams," *Engineering Structures*, **33**(3): 1025–1033.

GB50010-2010 (2010), *Code for Concrete Design of Structure*, Beijing: China Building Industry Press. (in Chinese)

GB50011-2010 (2010), *Code for Seismic Design of Buildings*, Beijing: China Building Industry Press. (in Chinese)

JGJ/T240-2011 (2011), *Technical Specification for Application of Recycled Aggregate*, Beijing: China Building Industry Press. (in Chinese)

Sato R, Maruyama I, Sogabe T and Sogo M (2007), "Flexural Behavior of Reinforced Recycled Aggregate Concrete Beam," *Journal of Advanced Concrete Technology*, **5**(1):43–61.

Sun YD, Xiao JZ, Zhou DY and Zhang P (2006), "An Experimental Study on the Seismic Behavior of Recycled Concrete Frames," *China Civil Engineering Journal*, **39** (5):9–15. (in Chinese)

Tabsh SW and Abdelfatah AS (2007), "Influence of Recycled Concrete Aggregates on Strength Properties of Concrete," *Construction and Building Materials*, **3**(2): 1163–1167.

Tam VWY (2009), "Comparing the Implementation of Concrete Recycling in The Australian and Japanese Construction Industries," *Journal of Cleaner Production*, **17**: 688–702.

Wang JC and Chen YK (2006), *Application of ABAQUS in Civil Engineering*, Zhejiang University Press. (in Chinese)

Xiao JZ and Falkner H (2007), "Bond Behaviour between Recycled Aggregate Concrete and Steel Rebars," *Construction and Building Materials*, **21**: 395–401.

Xiao JZ and Lan Y (2006), "An Experimental Study on Recycled Concrete Beams Flexural Performance," *Special Structures*, **23**(1): 9–12. (in Chinese)

Xiao JZ, Li JB and Zhang C (2005), "Mechanical Properties of Recycled Aggregate Concrete under Uniaxial Loading," *Cement and Concrete Research*, **35**: 1187–1194.

Xiao JZ, Li WG, Fan YH and Xiao H (2012), "An Overview of Study on Recycled Aggregate Concrete in China," *Construction and Building Materials*, **31**: 364–383.

Xiao JZ, Shen HB and Huang YB (2006), "Test on Compression Performance of Recycled Concrete Columns," *Structural Engineers*, **22**(6): 73–77. (in Chinese)

Xiao JZ and Zhu XH (2005), "Study on Seismic Behavior of Recycled Concrete Frame Joints," *Journal of Tongji University*, **33**(4): 436–440. (in Chinese)

Zhang JW, Cao WL, Dong HY and Zhu H (2010), "Experimental Study on Seismic Behavior of Mid-rise Recycled Concrete Shear Walls with Different Percentage of Aggregate Replacement," *China Civil Engineering Journal*, **43**(S2):55-–61. (in Chinese)

Zhuang Z, You XC, Liao JH, Cen S, Shen XP and Liang MG (2009), *FEM Analysis and Application Based on ABAQUS*, Beijing: Tsinghua University Press. (in Chinese)